



HAL
open science

A two time-scale model for tidal bed-load transport

Stéphane Cordier, Carine Lucas, Jean de Dieu Zabsonré

► **To cite this version:**

Stéphane Cordier, Carine Lucas, Jean de Dieu Zabsonré. A two time-scale model for tidal bed-load transport. *Communications in Mathematical Sciences*, 2012, 10 (3), pp.875-888. hal-00598932v1

HAL Id: hal-00598932

<https://hal.science/hal-00598932v1>

Submitted on 7 Jun 2011 (v1), last revised 10 Apr 2012 (v2)

HAL is a multi-disciplinary open access archive for the deposit and dissemination of scientific research documents, whether they are published or not. The documents may come from teaching and research institutions in France or abroad, or from public or private research centers.

L'archive ouverte pluridisciplinaire **HAL**, est destinée au dépôt et à la diffusion de documents scientifiques de niveau recherche, publiés ou non, émanant des établissements d'enseignement et de recherche français ou étrangers, des laboratoires publics ou privés.

A TWO TIME-SCALE MODEL FOR TIDAL BED-LOAD TRANSPORT [†]

STÉPHANE CORDIER [‡], CARINE LUCAS [§], AND JEAN DE DIEU ZABSONRÉ [¶]

Abstract. The goal of this article is to write a multi-scale analysis for a sedimentation model, namely a bed-load transport model. As this issue can be very difficult and expensive from a numerical point of view, the idea of the present work is to get a simplified model, satisfied by the first orders of our variables (in terms of asymptotic development), that can be easily implemented. This model is then validated on a numerical test of a dune in an ocean, submitted to tidal effects.

Key words. Shallow-Water Equations, bed-load transport, Exner equation, asymptotic developments, non-dimensional form, limit model, finite volumes scheme.

subject classifications. 34E13, 74S10, 65M06.

1. Introduction Developments in modeling bed-load transport are crucial to improve the prediction of water flows. Erosion phenomena (such as transport or sedimentation) can modify the human way of life, for example one can think about mudslides that may occur when it's raining for a long time. Erosion is not only due to rain, but it is also related to the oceans. On some coasts, numerous scientific studies aim at limiting disappearance of sand that weaken coastal installations, see among others [2, 1]. Coastal erosion is linked to water flow, and also to tides that increase the movements of the sea twice a day.

In this article, we consider the matter of the evolution of the topography in oceans, indeed in shallow water and submitted to the effects of tides. To this end, we couple Exner Equation for bed-load transport with Shallow-Water Equations and we perform a multi-scale analysis in time for this model. Several works have been led on this theme, see for example [7, 9, 10], but with the point of view of the stability analysis, or [5] for some recent existence results. The idea of the present work is to get a simplified model, satisfied by the first orders of our variables. This limit model is compared to the “reference solution”, given by a finite volume scheme on the full model (which can be very intricate). The comparison between these two models gives the price to pay to have a simple system, that can be easily programmed.

More precisely, the outline of the present paper is the following: in Section 2, we explain the obtention of the model. We begin writing the Shallow-Water Equations, to get the evolution of the fluid, and the classical Exner Equation, for the evolution of the topography. We have to choose one of the empirical expressions for the sediment discharge in the bed-load transport model and we obtain our complete model. Then we introduce non-dimensional variables and parameters to get the non-dimensional equations and be able to perform the asymptotic analysis. Our new simplified model is obtained combining the first orders of the asymptotics. In section 3, we explain the way we implemented the complete model, with a finite volume scheme. We also

*This work has been partially supported by the project METHODE 566 ANR-07-BLAN-0232

[†]Received date / Revised version date

[‡]MAPMO UMR CNRS 6628, Université d'Orléans, Bâtiment de mathématiques, B.P. 6759 - 45067 Orléans cedex 2, France, (cordier@math.cnrs.fr).

[§]MAPMO UMR CNRS 6628, Université d'Orléans, Bâtiment de mathématiques, B.P. 6759 - 45067 Orléans cedex 2, France, (carine.lucas@univ-orleans.fr).

[¶]ISEA, Université Polytechnique de Bobo-Dioulasso, 01 B.P. 1091 Bobo 01, Burkina Faso, (jzabsonre@gmail.com).

compute the solutions of our new (and simple) limit model and we compare their results; the test case is a dune, initially at rest, but that oscillates with tidal effects. To improve the comparison, we introduce two variables related to the topography that describe the way the dune spreads.

2. Derivation of the model We start this study with the derivation of the model: we consider the Shallow-Water Equations coupled with the Exner equation for the evolution of the bed. We introduce non-dimensional variables in order to make an asymptotic analysis and obtain an approximate solution of the complete model.

2.1. Equations for bed-load transport The first point is to write equations modelling the transport of sediments, in a shallow domain. Usually, the Shallow-Water Equations (SWE) are coupled with a transport equation on the sediment height. More precisely, we can define the following variables (see Figure 2.1):

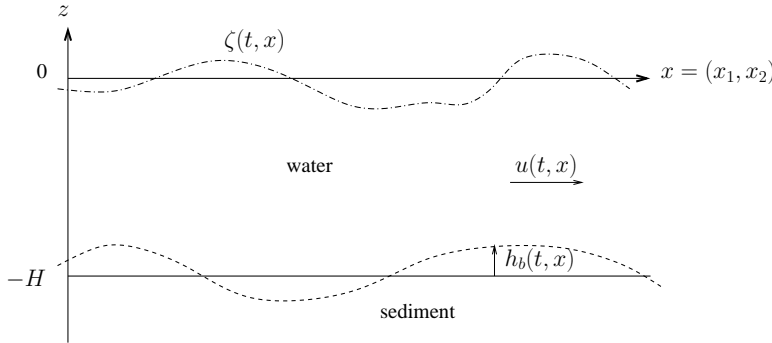


FIG. 2.1. *Sediment layer and water with free surface*

H is the mean water height on the domain, u the velocity of the fluid, and ζ is the function that describes the free surface. The function h_b denotes the sediment height starting from the level $z = -H$.

With these notations, the Shallow-Water Equations (SWE) are given by:

$$\partial_t(\zeta - h_b) + \operatorname{div}((\zeta + H - h_b)u) = 0, \quad (2.1a)$$

$$\begin{aligned} \partial_t((\zeta + H - h_b)u) + \operatorname{div}((\zeta + H - h_b)u \otimes u) + \\ g(\zeta + H - h_b)\nabla\zeta + f(\zeta + H - h_b)u^\perp = -ku, \end{aligned} \quad (2.1b)$$

where g is the gravity, f the Coriolis term, k the friction coefficient, and $u^\perp = {}^t(-u_2 \ u_1)$ if u_1 and u_2 are the two components of the water velocity field u .

SWE (2.1) must be coupled with a bed-load evolution: for the sediment transport, several formulations of the classical Exner equation are given in the literature, depending on the sediment properties. We can mention here Van Rijn and Meyer-Peter and Müller (MPM) formulations, cf. [11] for example. In our case, we choose a simple expression, such as the one given by Grass [6]:

$$\partial_t h_b + A \operatorname{div}(u^3) = 0, \quad (2.2)$$

where A is a coefficient given by the sediment characteristics (usually small).

In the following, our objective is to study the coupling between Equations (2.1) and (2.2).

2.2. Choice of the scalings: non-dimensional quantities As we consider a domain such as an ocean, we have to take into account tides effects. Then two length scales coexist, namely L (the tidal wave length) and l (the tidal excursion length). If σ denotes the tidal frequency and U the tidal current amplitude, we have $l = U/\sigma$. We introduce non-dimensional variables, with a prime, given by:

$$u = Uu', \quad t = \frac{t'}{\sigma}, \quad x = lx', \quad h_b = Hh'_b, \quad \zeta = \frac{UL\sigma}{g}\zeta'.$$

The scaling on ζ is linked to the typical momentum balance for a tidal wave.

We can introduce the small parameter δ , which is the ratio between l and L ($\delta \approx 10^{-3}$). This parameter δ can also be written as $\delta = U/(\sigma L)$, which means, considering the dispersion relation $L\sigma = \sqrt{gH}$, that the scaling on ζ reads:

$$\zeta = \delta H \zeta', \quad \text{with} \quad \delta = \frac{l}{L} = \frac{U}{\sigma L}.$$

Last, we must define some non-dimensional parameters

$$A' = \frac{AU^3}{l\sigma H}, \quad f' = \frac{f}{\sigma}, \quad k' = \frac{k}{H\sigma}$$

to simplify the writing of the equations.

2.3. Non-dimensional equations We replace the previous relations in Equations (2.1)–(2.2); dropping the primes, we get the following non-dimensional relations:

$$\begin{aligned} \delta \partial_t \zeta - \partial_t h_b + \delta \operatorname{div}(\zeta u) + \operatorname{div}(u - h_b u) &= 0, \\ \partial_t((\delta \zeta + 1 - h_b)u) + \operatorname{div}((\delta \zeta + 1 - h_b)u \otimes u) + \\ &\quad \frac{1}{\delta}(\delta \zeta + 1 - h_b)\nabla \zeta + f(\delta \zeta + 1 - h_b)u^\perp = -ku, \\ \partial_t h_b + A \operatorname{div}(u^3) &= 0. \end{aligned}$$

As A is a small parameter (of order of δ^2), we can define a new time scale:

$$\tau = At,$$

and we assume h_b to be a function of τ and x only. Then we can rewrite the non-dimensional equations as:

$$\delta \partial_t \zeta + \delta A \partial_\tau \zeta - A \partial_\tau h_b + \delta \operatorname{div}(\zeta u) + \operatorname{div}(u - h_b u) = 0, \quad (2.3a)$$

$$\begin{aligned} \partial_t((\delta \zeta + 1 - h_b)u) + A \partial_\tau((\delta \zeta + 1 - h_b)u) + \operatorname{div}((\delta \zeta + 1 - h_b)u \otimes u) \\ + \frac{1}{\delta}(\delta \zeta + 1 - h_b)\nabla \zeta + f(\delta \zeta + 1 - h_b)u^\perp = -ku, \end{aligned} \quad (2.3b)$$

$$\partial_\tau h_b + \operatorname{div}(u^3) = 0. \quad (2.3c)$$

In order to study these relations, we perform an asymptotic development in powers of δ .

2.4. Asymptotic development We decompose our variables in powers of δ :

$$\begin{aligned}\zeta &= \zeta^0 + \delta\zeta^1 + \delta^2\zeta^2 \dots \\ h_b &= h_b^0 + \delta h_b^1 + \delta^2 h_b^2 \dots \\ u &= u^0 + \delta u^1 + \delta^2 u^2 \dots\end{aligned}$$

We replace these relations into Equations (2.3) and we identify the powers of δ . At the first order, we find:

$$\begin{aligned}\operatorname{div}(u^0 - h_b^0 u^0) &= 0, \\ \nabla \zeta^0 &= 0, \\ \partial_\tau h_b^0 + \operatorname{div}\left((u^0)^3\right) &= 0,\end{aligned}$$

and at the second order, we get the evolution of u^0 :

$$\begin{aligned}\partial_t \zeta^0 + \operatorname{div}(\zeta^0 u^0) + \operatorname{div}(u^1 - h_b^1 u^0 - h_b^0 u^1) &= 0, \\ (1 - h_b^0) \partial_t u^0 + \operatorname{div}\left((1 - h_b^0) u^0 \otimes u^0\right) + (1 - h_b^0) \nabla \zeta^1 + f(1 - h_b^0) u^{0\perp} &= -k u^0, \\ \partial_\tau h_b^1 + 3 \operatorname{div}\left(u^{02} u^1\right) &= 0.\end{aligned}$$

2.5. Model The study of the first orders shows that ζ^0 is a function of t only, given by the boundary conditions. The evolutions of u^0 and h_b^0 satisfy:

$$\operatorname{div}(u^0 - h_b^0 u^0) = 0, \tag{2.4a}$$

$$\partial_\tau h_b^0 + \operatorname{div}\left((u^0)^3\right) = 0, \tag{2.4b}$$

$$\begin{aligned}(1 - h_b^0) \partial_t u^0 + \operatorname{div}\left((1 - h_b^0) u^0 \otimes u^0\right) + (1 - h_b^0) \nabla \zeta^1 \\ + f(1 - h_b^0) u^{0\perp} = -k u^0,\end{aligned} \tag{2.4c}$$

system that can be solved using finite elements and the augmented Lagrangian method, in order to be able to treat the term in ζ^1 .

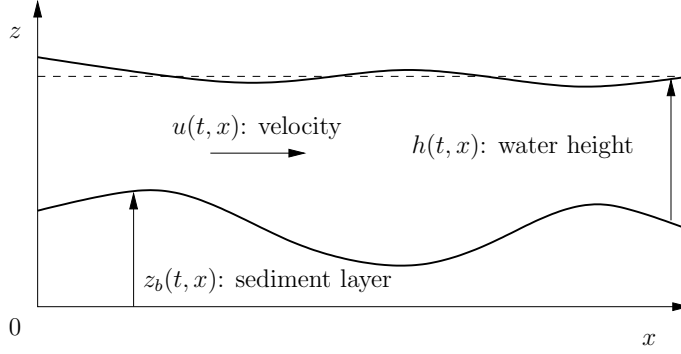
REMARK 2.1. *We could also introduce other space variables, namely $X = x/\delta$ and $\chi = \delta x$. In the first case, writing the equations, we find that the first order does not depend on X , and we get the same system as in Section 2.5 taking the mean value, in X of our equations.*

In the second case, we obtain a system of the same type as the one of Section 2.5 but instead of $\nabla \zeta^1$ we have $\nabla \zeta^1 + \nabla_\chi \zeta^0$, where ∇_χ is the gradient in the coordinates χ .

3. Numerical test In order to validate our new model, we compare the results given by a finite volumes scheme on the full equations (2.1)-(2.2) and the solution of (2.4) on a one dimensional test case. We consider a dune in the domain and we impose periodic boundary conditions on the velocity to simulate tides.

3.1. Finite volume scheme for the full model The first approach is to get a ‘‘reference solution’’, through the resolution of the full Shallow-Water-Exner equations (2.1)–(2.2). This problem has been studied for example by [3, 4] using a finite volumes scheme.

In order to keep the same notations as the one used in the above references, we do not consider notations of Figure 2.1 anymore but the one of Figure 3.1 (note that the variables are related through the relation $h = H + \zeta - h_b$).

FIG. 3.1. *Sediment layer and water with free surface for the finite volume scheme*

With these notations, in one dimension (without the Coriolis term) and without friction ($k=0$), Shallow-Water and Exner equations read:

$$\begin{aligned} \partial_t h + \partial_x(hu) &= 0, \\ \partial_t(hu) + \partial_x(hu^2) + g(h+z_b)\partial_x h &= 0, \\ \partial_t z_b + A\partial_x u^3 &= 0. \end{aligned} \quad (3.1)$$

System (3.1) can be written under the form $\partial_t W + A(W)\partial_x W = B(W)\partial_x W$, where $A(W) = \partial_W(F(W))$ is the jacobian matrix of F , being

$$W = \begin{bmatrix} h \\ q \\ z_b \end{bmatrix}, \quad F = \begin{bmatrix} q \\ \frac{q^2}{h} + \frac{1}{2}gh^2 \\ A\frac{q^3}{h^3} \end{bmatrix}, \quad B = \begin{bmatrix} 0 & 0 & 0 \\ 0 & 0 & -gh \\ 0 & 0 & 0 \end{bmatrix}.$$

The full Shallow-Water Exner system (3.1) can also be written:

$$\partial_t W + \mathcal{A}(W)\partial_x W = 0, \quad (3.2)$$

where $\mathcal{A}(W) = A(W) - B(W)$. Due to the definition of F we have the following expression for $\mathcal{A}(W)$:

$$\mathcal{A}(W) = \begin{bmatrix} 0 & 1 & 0 \\ -\frac{q^2}{h^2} + gh & 2\frac{q}{h} & gh \\ -3A\frac{q^3}{h^4} & 3A\frac{q^2}{h^3} & 0 \end{bmatrix}.$$

To simulate this model, we consider the finite volumes scheme developed in [3]. Let W_i^n be the average of W over the volume V_i at time t^n . We obtain the following numerical scheme :

$$W_i^{n+1} = W_i^n - \frac{dt}{dx} \left(\mathcal{D}_{i+1/2}^+ + \mathcal{D}_{i+1/2}^- \right),$$

with

$$\begin{aligned} \mathcal{D}_{i+1/2}^\pm &= \pm \frac{\alpha_0}{2} (W_{i+1}^n - W_i^n) \\ &\pm \left(\frac{1}{2} + \frac{\alpha_1}{2} \right) (F(W_{i+1}^n) - F(W_i^n) - B_{i+1/2}(W_{i+1}^n - W_i^n)) \\ &\pm \frac{\alpha_2}{2} \mathcal{A}_{i+1/2} (F(W_{i+1}^n) - F(W_i^n) - B_{i+1/2}(W_{i+1}^n - W_i^n)), \end{aligned}$$

where $\mathcal{A}_{i+1/2}$ is the Roe linearization matrix. The coefficients α_i are given by the formulas:

$$\begin{aligned}\alpha_0 &= \frac{|\lambda_1|\lambda_2\lambda_3}{(\lambda_2-\lambda_1)(\lambda_3-\lambda_1)} + \frac{|\lambda_2|\lambda_1\lambda_3}{(\lambda_1-\lambda_2)(\lambda_3-\lambda_2)} + \frac{|\lambda_3|\lambda_1\lambda_2}{(\lambda_3-\lambda_1)(\lambda_3-\lambda_2)}, \\ \alpha_1 &= -\lambda_1 \left(\frac{|\lambda_2|}{(\lambda_1-\lambda_2)(\lambda_3-\lambda_2)} + \frac{|\lambda_3|}{(\lambda_1-\lambda_3)(\lambda_2-\lambda_3)} \right) \\ &\quad -\lambda_2 \left(\frac{|\lambda_1|}{(\lambda_2-\lambda_1)(\lambda_3-\lambda_1)} + \frac{|\lambda_3|}{(\lambda_1-\lambda_3)(\lambda_2-\lambda_3)} \right) \\ &\quad -\lambda_3 \left(\frac{|\lambda_1|}{(\lambda_2-\lambda_1)(\lambda_3-\lambda_1)} + \frac{|\lambda_2|}{(\lambda_3-\lambda_2)(\lambda_1-\lambda_2)} \right), \\ \text{and} \\ \alpha_2 &= \frac{|\lambda_1|}{(\lambda_2-\lambda_1)(\lambda_3-\lambda_1)} + \frac{|\lambda_2|}{(\lambda_1-\lambda_2)(\lambda_3-\lambda_2)} + \frac{|\lambda_3|}{(\lambda_3-\lambda_1)(\lambda_3-\lambda_2)},\end{aligned}$$

where the coefficients λ_i , (for $i=0,1,2$) are the eigenvalues of the matrix $\mathcal{A}_{i+1/2}$, see [4].

3.2. Numerical results We consider the spatial domain $[0,20]$, discretized with 100 points. In this domain, we impose an initial dune, given by:

$$z_b(t=0, x) = b_0 + \max(0.1 - 0.05(x-10)^2, 0), \quad \text{with } b_0 = 0.1$$

see Figure 3.2.

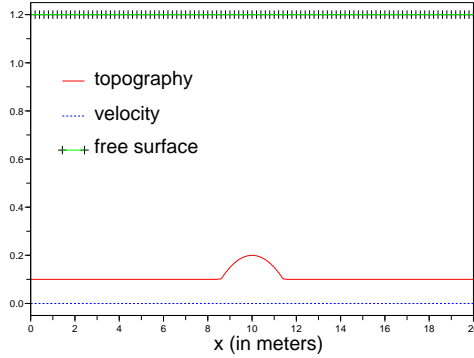


FIG. 3.2. *Initial conditions*

In order to have a constant free surface, we choose a low velocity with periodic condition on the boundaries $x=0$ and $x=20$, namely:

$$u(t, x=0) = u(t, x=20) = 5.4 \sin(\pi t/6), \quad \text{in m/h.}$$

The variable t is the time expressed in hours, such that there are two periods a day. We assume that at the initial time, the velocity is null: $u(t=0, x) = 0$ such that the initial conditions are given by Figure 3.2. For these choices of initial conditions and velocity, the free surface stays flat without moving.

Let us explain the results we obtained. First, we present the evolution of the bottom at the times $t=3, 6, 12, 18, 24, 30, 36, 48$ hours respectively in Figure 3.3,

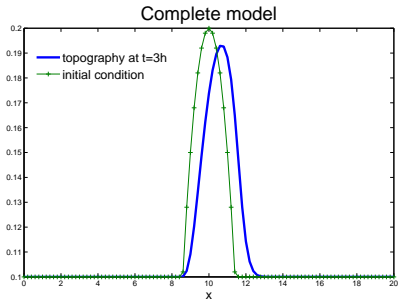
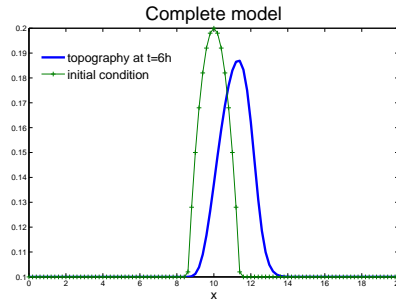
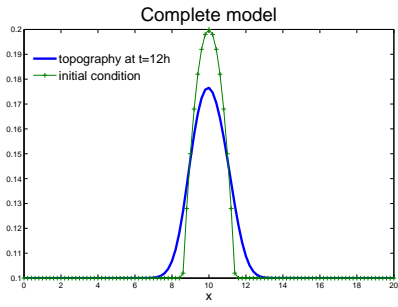
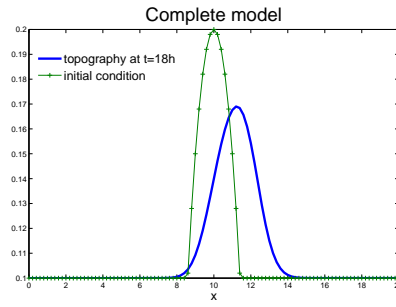
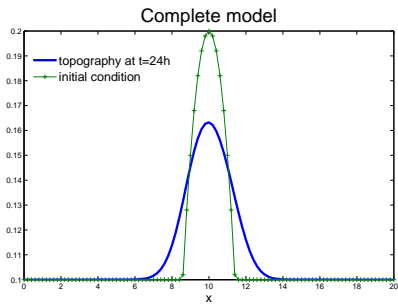
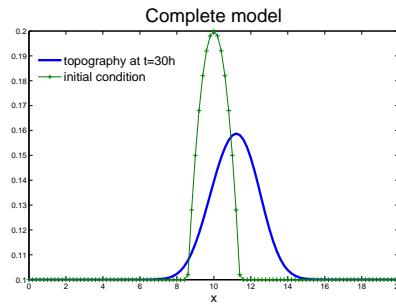
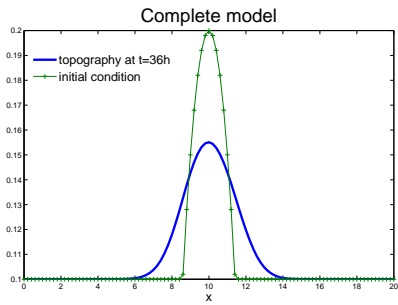
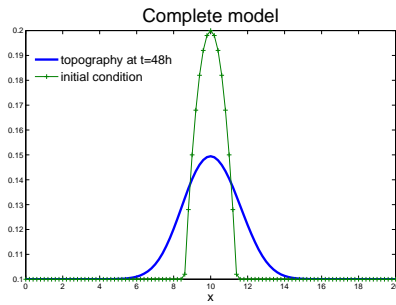
(a) $t = 3$ h.(b) $t = 6$ h.(c) $t = 12$ h.(d) $t = 18$ h.(e) $t = 24$ h.(f) $t = 30$ h.(g) $t = 36$ h.(h) $t = 48$ h.

FIG. 3.3. Evolution of the topography with the complete model (100 points)

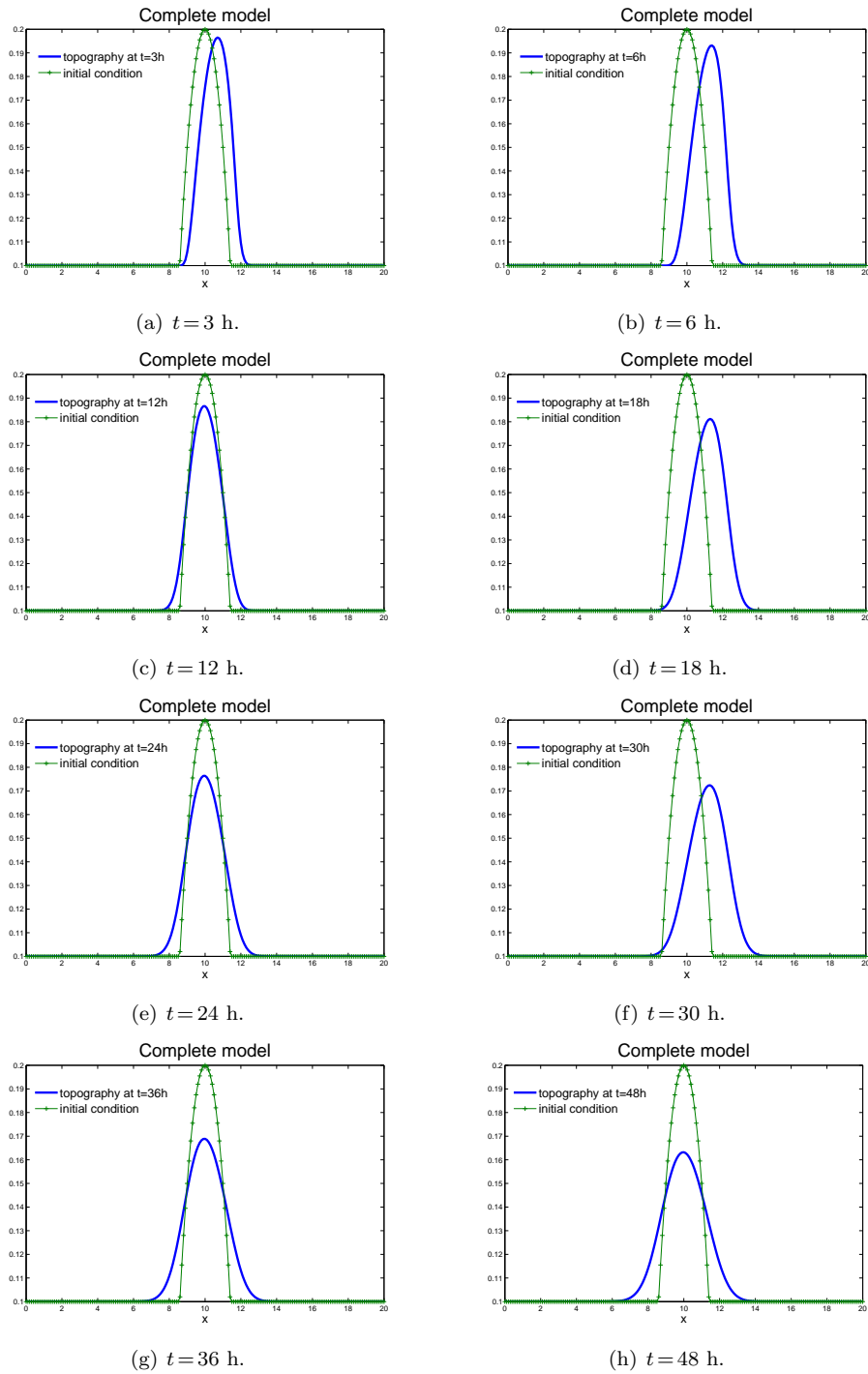


FIG. 3.4. Evolution of the topography with the complete model (200 points)

solution of system (3.1) with $A=0.001$. One can notice that the dune is moving towards the right or the left, depending on the sign of the velocity. At the same time, the dune is spreading.

In Figures 3.4, we plotted the results obtained with the complete model by using a finer grid. Instead of the space step dx , we took $\frac{dx}{2}$. Comparing the results obtained in these configurations, we can assert that the displacement of the dune is not only due to this numerical diffusion.

To improve the comparison between the two models (full Shallow Water system with Exner equation and the simplified limit model), we consider the two following functions (of time):

$$Z(t) = \max_{0 \leq x \leq L} z_b(x, t) \quad \text{and} \quad N(t) = \text{card} \left\{ i \text{ s.t. } z_b(x_i, t) \geq \frac{Z(t) - b_0}{2} + b_0 \right\}.$$

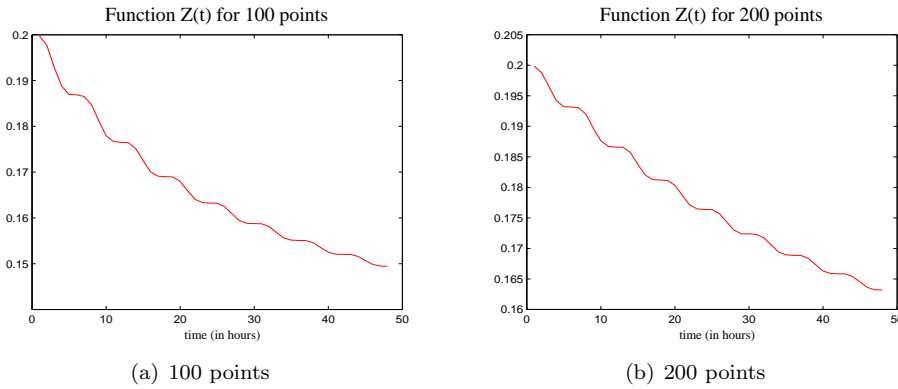


FIG. 3.5. Graphs of the function $Z(t)$

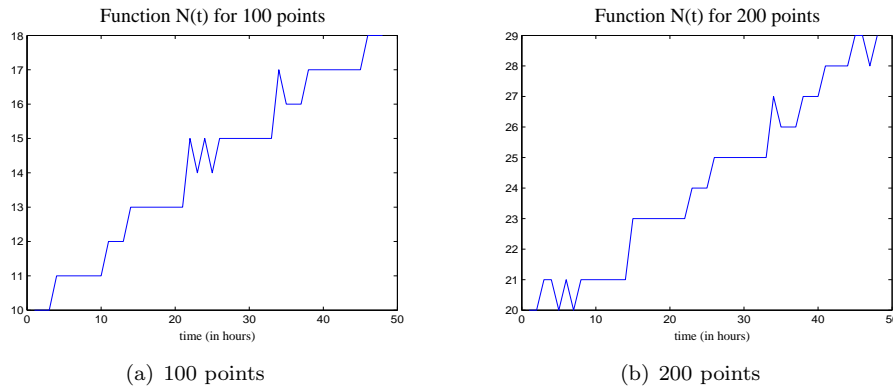


FIG. 3.6. Graphs of the function $N(t)$

The first function Z represents the evolution in time of the maximum of the dune, and the second function N characterizes the spread of the dune.

The results are plotted in Figures 3.5-3.6 (the sawtooth shape of the function N is due to the integer values of $N(t)$ and to the discrete values of the time, every one hour).

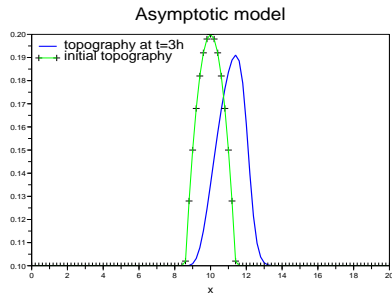
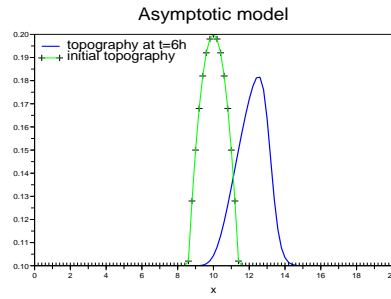
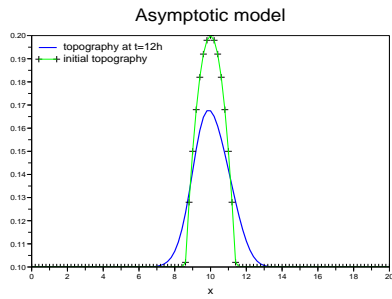
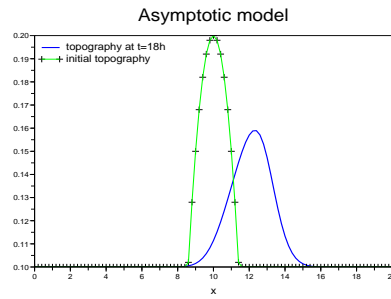
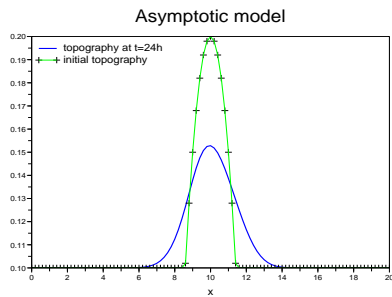
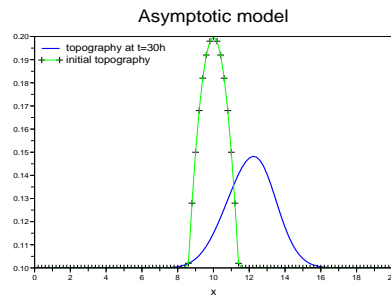
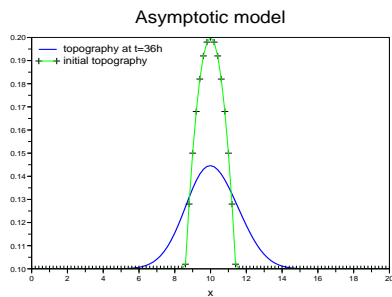
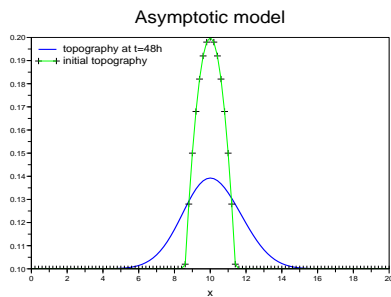
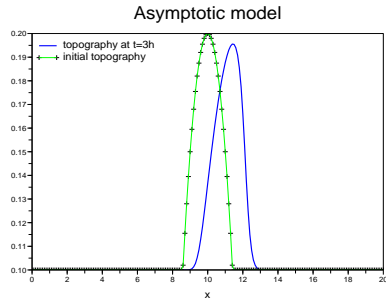
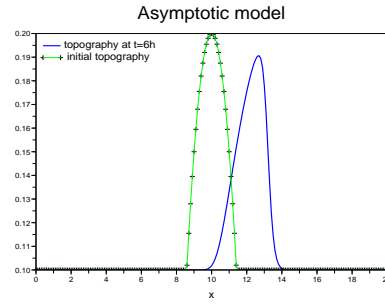
(a) $t = 3$ h.(b) $t = 6$ h.(c) $t = 12$ h.(d) $t = 18$ h.(e) $t = 24$ h.(f) $t = 30$ h.(g) $t = 36$ h.(h) $t = 48$ h.

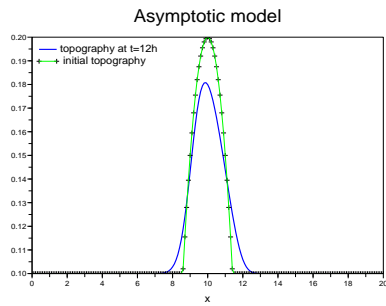
FIG. 3.7. Evolution of the topography with the asymptotic model (100 points)



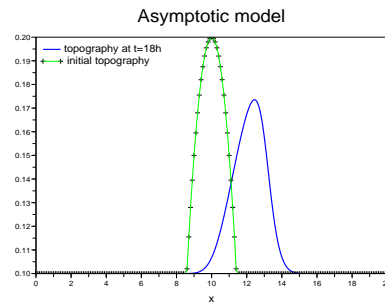
(a) $t = 3$ h.



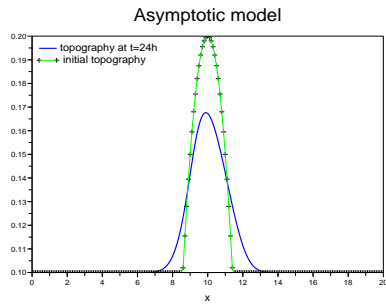
(b) $t = 6$ h.



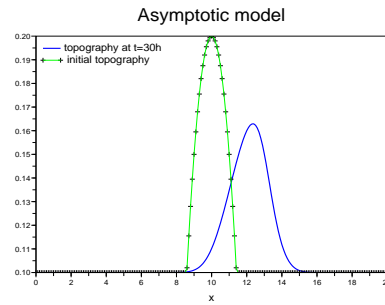
(c) $t = 12$ h.



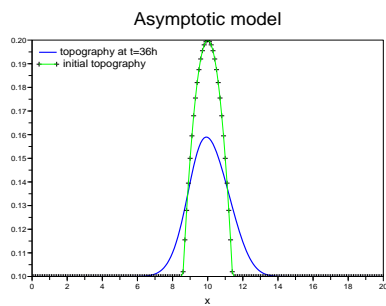
(d) $t = 18$ h.



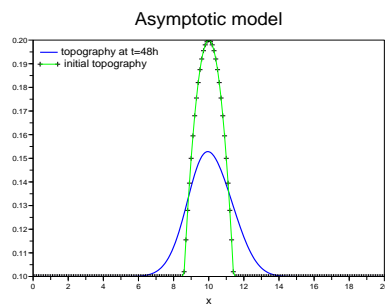
(e) $t = 24$ h.



(f) $t = 30$ h.



(g) $t = 36$ h.



(h) $t = 48$ h.

FIG. 3.8. Evolution of the topography with the asymptotic model (200 points)

Let us now compare the solutions of the two systems.

First one may notice that for 100 points, the complete model needs nearly one hour, with 200 points, the computation time is about several hours, whereas the limit model takes a few seconds.

For the asymptotic model, we plotted in Figure 3.7 the solutions of (2.4) at $t=3, 6, 12, 18, 24, 30, 36, 48$ hours respectively for 100 points. In Figure 3.8, the space step is divided by 2. Comparing with Figures 3.3-3.4 for the full model, we conclude that our new simplified system gives good results, but the computation time is much smaller than for the complete model.

Last, in Figures 3.9-3.10, one can compare the functions Z and N for the limit model, still very similar to results for the full model.

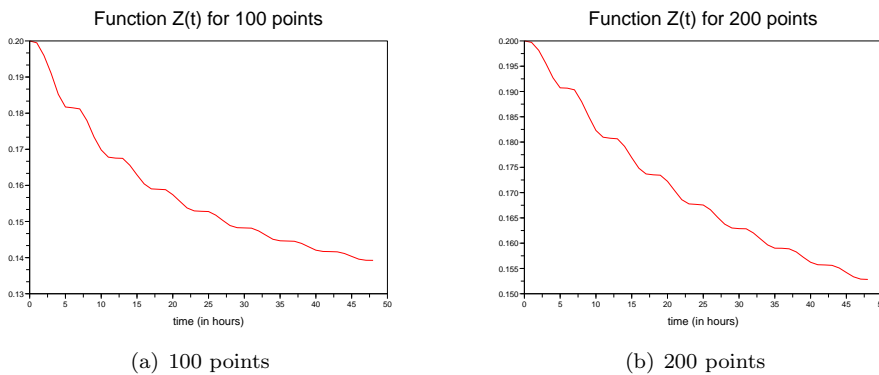


FIG. 3.9. *Graphs of the function $Z(t)$*

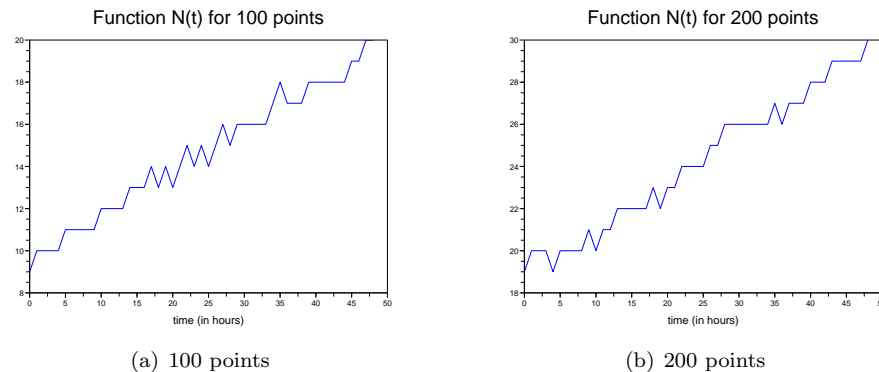


FIG. 3.10. *Graphs of the function $N(t)$*

The first conclusion we can give with these numerical results is that the simplified limit model behaves very well compared to the complete model, but the computation time is very lower.

3.3. More numerical results In this part, we focus our attention on the spreading on the dune, in both models. To that end, we consider several space steps:

$dx = 0.2, \frac{dx}{2}, \frac{dx}{4}$ and $\frac{dx}{8}$. Our goal is to quantify the effects of the numerical diffusion.

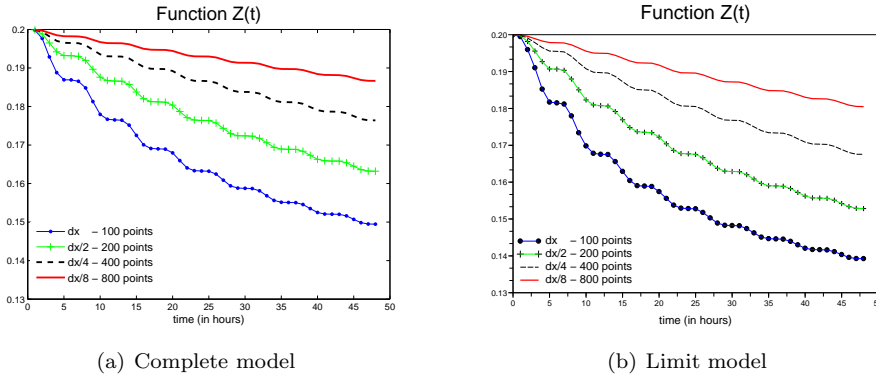


FIG. 3.11. Graphs of the functions $Z(t)$

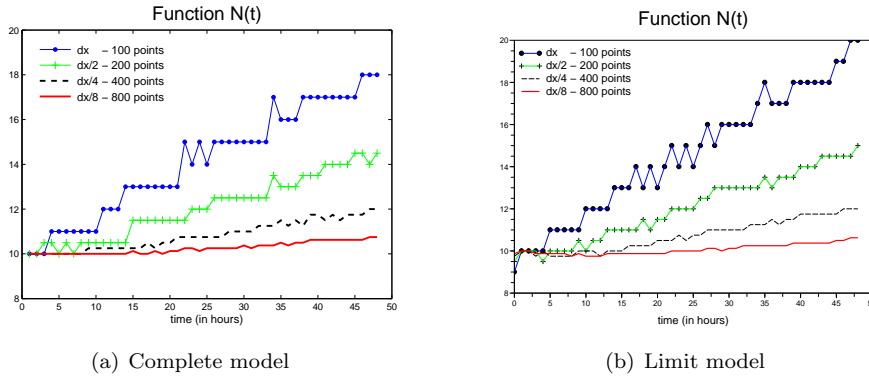


FIG. 3.12. Graphs of the functions $N(t)$

In Figures 3.11-3.12, we plotted the functions Z and N for the various space steps, for the complete and the limit model. (Functions N are rescaled to take into account the number of points). As explained before, the two models have the same behavior but this is not the point we want to emphasize. These figures and Figures 3.3-3.4, 3.7-3.8 show that the x -coordinate of the culmination of the dune does not depend of the space step (the movement due to tides is well reproduced by the two models). However, in both cases, the height of the culmination point is linked to the value of the space step: the diffusion that makes the dune spread is only numerical diffusion, even if it seems “natural”. This means that the diffusion of the topography is not modeled in the complete system (2.1)-(2.2) (and consequently in the limit model).

4. Conclusions In this paper, we performed asymptotic developments in order to decouple the two time scales that appear in the oceans, considering the effect of tides. We obtained a new model and we carried out some experiments. Comparisons with the complete model give good results in one dimension, with the advantage that

our new limit model is much faster (a few seconds compared to a few hours) and easier to implement than the complete one.

However, the spreading of the dune is only due to the numerical diffusion, which means that, in the Shallow-Water system with Exner equation considering Grass flow, there is no diffusion of the evolution of the topography. This is contrary to the observations one can make, and we can suggest to add diffusive terms in the Exner equation, as in [12] for example, or [8] for Meyer-Peter and Müller equation.

The numerical validation of these results is still in progress in the two dimensional case.

Acknowledgments. As this work started with a French-American collaboration, the second author would like to thanks the “Equipes Associées” program of INRIA (between J. McWilliams’s team (UCLA) and Moise INRIA team (Grenoble, France), directed by E. Blayo) which partly funded this work.

The third author is partially supported by the AUF, and is very grateful to the MAPMO laboratory for the accommodation he get.

REFERENCES

- [1] P. AZERAD, F. BOUCHETTE, D. ISEBE, B. MOHAMMADI, Shape optimization of geotextile tubes for sandy beach protection, *International Journal for Numerical Methods in Engineering*, 74: 1262–1277, 2008.
- [2] A. BOUHARGUANE, B. MOHAMMADI, Minimization principles for the evolution of a soft sea bed interacting with a shallow sea, *submitted*.
- [3] J. M. CASTRO, E. D. FERNÁNDEZ-NIETO, A class of computationally fast first order finite volumes solvers. *PVM Methods*, *submitted*.
- [4] J. M. CASTRO, E. D. FERNÁNDEZ-NIETO, A. FERREIRO-FERREIRO, Sediment transport models in Shallow Water, *Computers & Fluids*, 37(3): 299–316, 2008.
- [5] I. FAYE, E. FRENOD, D. SECK, Singularly perturbed degenerated parabolic equations and application to seabed morphodynamics in tided environment, *Discrete and Continuous Dynamical Systems: Series A*, 29(3): 1001-1030, 2011.
- [6] A. J. GRASS, Sediment transport by waves and currents, *Technol. Report No.: FL29*, SERC London, Cent. Mar., 1981.
- [7] S. HULSCHER, Formation and migration of large-scale, rhythmic sea-bed patterns: a stability approach, *Ph.D. thesis*, Utrecht University, 1996.
- [8] T. MORALES DE LUNA, M. J. CASTRO DÍAZ, C. PARÉS MADROÑAL, A duality method for sediment transport based on a modified Meyer-Peter&Müller model, *Journal of Scientific Computing*, DOI: 10.1007/s10915-010-9447-1 .
- [9] P. C. ROOS, Seabed Pattern Dynamics and Offshore Sand Extraction, *Ph.D. thesis*, University of Twente, 2004.
- [10] H. SCHUTTELAARS, Evolution and Stability Analysis of Bottom Patterns in Tidal Embayements, *Ph.D. thesis*, Utrecht University, 1997.
- [11] R. SOULSBY, Dynamics of marine sands: a manual for practical applications, *Thomas Telford*, London, 1997.
- [12] J. de D. ZABSONRÉ, C. LUCAS, E. FERNÁNDEZ-NIETO, An Energetically Consistent Viscous Sedimentation Model, *Mathematical Models and Methods in Applied Sciences*, 19(3): 477–499, 2009.